31st Annual International Conference of the IEEE EMBS
Minneapolis, Minnesota, USA, September 2-6, 2009

Towards Cardiovascular Risk Stratification Using Imaging Data

I.A. Kakadiaris, *Senior Member, IEEE*, U. Kurkure, E.G. Mendizabal-Ruiz, and M. Naghavi

Abstract— **In spite of the advancement and proliferation of cardiovascular imaging data, the rate of deaths due to unpredicted heart attack remains high. Thus, it becomes imperative to develop novel computational tools to mine quantitative parameters from imaging data for early detection and diagnosis of asymptomatic cardiovascular disease. In this paper, we present our progress towards developing a computational framework to mine cardiac imaging data and provide quantitative measures for developing a new risk assessment method. Specifically, we present computational methods developed for the detection of coronary calcification and segmentation of thoracic aorta in non-contrast cardiac computed tomography, and detection of neovessels in plaques in intravascular ultrasound imaging data.**

I. INTRODUCTION

The National Heart Lung and Blood Institute reported that 872,000 deaths or 36% of all deaths in the United States were due to cardiovascular disease in 2004 [1]. Approximately 50% of heart attack related deaths occur in people with no prior symptoms. Hence, sudden heart attack remains the number one cause of death in the US. Unpredicted heart attacks account for the majority of the $280 billion burden of cardiovascular diseases. The field of cardiology has witnessed a major paradigm shift in its determination of a patient's risk of coronary artery disease. Today, cardiovascular specialists know that heart attacks are caused by inflammation of the coronary arteries and thrombotic complications of vulnerable plaques. As a result, the discovery of vulnerable plaque has recently evolved into the definition of "vulnerable patient". *A vulnerable patient is defined as a person with more than a 10% likelihood of having a heart attack in the next 12 months*. Over 45 world leaders in cardiology have collectively introduced the field of vulnerable patient detection as defining the new era in preventive cardiology [2], [3].

Existing cardiovascular risk scoring methods do not take into account the wealth of information that is available in imaging data. The reason for this is two-fold: 1) there is a dearth of automatic techniques to mine the data for required information, and 2) validation in large epidemiological studies is needed to determine which type of information will offer additive predictive value. Our long-term vision is to contribute to the development of quantitative methods to assess cumulative risk of vulnerable patients by developing new techniques to mine additional information from imaging data.

I.A. Kakadiaris, U. Kurkure and E.G. Mendizabal are with the Computational Biomedicine Lab, Department of Computer Science, University of Houston, 4800 Calhoun Rd., Houston, TX 77204-3010 USA (ioannisk@uh.edu, ukurkure, egmendiz@uh.edu).

M. Naghavi is with the Society for Heart Attack Prevention and Eradication (SHAPE), Houston, TX.

Several studies have established that the presence of calcified coronary plaque as detected by computed tomography (CT) has a significant predictive value for coronary artery disease in both asymptomatic and symptomatic patients, and is associated with future cardiac events [4], [5], [6], [7]. Coronary calcification burden has been reported to be associated with cardiovascular risk. Currently, an observer must identify the coronary calcifications among a set of candidate regions (obtained by thresholding and connected component labeling) by clicking on them. To relieve the observer of such a labor-intensive task, an automated tool is needed that can detect and quantify the coronary calcifications. However, the diverse and heterogeneous nature of the candidate regions poses a significant challenge to the accurate detection of coronary calcifications. Studies have also shown that calcification of the thoracic aorta, aortic arch and aortic valve are associated with increased risk of cardiovascular disease [8], [9]. Thoracic aorta calcification can be measured from standard cardiac CAC scans without requiring any additional scanning, which is especially advantageous for retrospective studies. However, there are no automated methods that address the problem of aorta segmentation in non-contrast cardiac CT scans. This may be attributed to the nature of the non-contrast CT imaging, which suffers from lack of contrast between blood pool regions, muscle walls and pericardial fat, rendering the aorta segmentation quite a challenging task.

Furthermore, vasa vasorum (VV) neovascularization on the plaque has been identified as a common feature of inflammation [10] and has being defined as a plaque vulnerability index. Intravascular ultrasound (IVUS) is currently the gold-standard technique for assessing the morphology of blood vessels and atherosclerotic plaques *in vivo*. IVUS combined with contrast-enhancing agents as blood tracer has been used for the detection of blood perfusion within the vessel. The method involves injecting high-echogenic microbubbles of size similar to red blood cells into the blood flow while monitoring with IVUS. If these microbubbles are found beyond the lumen border, this could be an indication of microcirculation due to VV. However, manually performing temporal analysis of variations in wall echogenicity is not feasible. Computer-aided techniques may be a natural solution to this problem, though they present their own difficulties.

II. METHODS

A. Computed Tomography

We have developed a novel two-stage hierarchical classification-based method to detect coronary calcifications

in non-contrast cardiac CT scans [11]. In this classification problem, the positive class is composed of the coronary calcifications, while the negative class consists of the aortic calcifications, image noise, and metal implants, if any. Figure 1 depicts the typical candidate regions for the coronary and aortic calcifications as well as the image noise. In the first stage, the arterial (the coronary and the aortic) calcifications are distinguished from other highly dense regions present within the heart region. In the second stage, the coronary calcifications are distinguished from the aortic calcifications. We investigated the possibility of such separation without requiring the segmentation of the aorta. At each stage of the hierarchy, we constructed an ensemble of classifiers whose decisions are combined to obtain the final decision for that stage. Each classifier in the ensemble was designed to accommodate asymmetric penalty costs for different types of errors.

Fig. 1. CT image of a heart depicting typical candidates from the positive and the negative class - coronary calcifications in LAD (A), RCA (B), aorta (C), and image noise (D,E).

Though the coronary calcifications appear as high-density structures in the non-contrast CT scans, it is inherently difficult to identify them automatically. The difficulty arises because of the presence of other similar high-density structures, including the non-coronary calcifications and the absence of any contrast agent to identify the blood vessels. It is apparent that the choice of features plays an important role in solving this problem. We have investigated various clues that a human observer uses to manually annotate the coronary calcifications in the CT scans. Thus, we have computed the relative location of the calcifications with respect to a heart-centered coordinate system and used the neighboring region of the calcifications to better characterize their properties for discrimination.

Our results demonstrated the feasibility of an automated coronary calcium detection system using a classification-based method and that a heart-centered coordinate system provides a compact representation for the spatial location of the coronary arteries, as opposed to the absolute image coordinate system. Initially, we used a simple bounding box-based coordinate system to represent the location of the calcifications. Development of a more compact frame of reference using a local heart-centered coordinate system, as recently proposed by our group [12], which is aligned in terms of translation, scale, and rotation, could further improve the accuracy of the calcification detection system. It has also been shown that the texture features characterize the coronary calcifications well, and the neighborhood region of the coronary calcium plays an important role in distinguishing coronary calcium from other candidate regions. Thus, the inclusion of the neighborhood region in the candidate region in order to compute the region-based texture features significantly improved the sensitivity of the system. Our method achieved sensitivity of 92.07% at the expense of 4.65 false positives per scan. Also, using an ensemble of multiple classifiers further reduced the false positives occurring due to image noise. Nevertheless, there is a high percentage of misclassification errors for the calcifications in the aorta, left main artery and right coronary artery. These misclassifications are due to the atomical variations in the relative positions of the ascending aorta near the origin, the left main artery and the proximal region of the right coronary artery in different subjects.

To this end, we have developed a novel method for segmentation of the thoracic aorta in non-contrast cardiac CT images and posterior quantification of aortic calcified plaque [13]. We used dynamic programming concepts to reformulate the problems of localizing and segmenting the thoracic aorta as optimal path detection problems constrained by certain cost functions. Our method consisted of the following steps. The first step was to locate the position and estimate the size of the aorta in the thoracic CT scans. In spite of heart dynamics, the aorta maintains its global tubular shape with minor local deformations. Since the thoracic aorta runs vertically, its appearance in axial slices approximates a circular shape which can be extracted using the Hough transform. However, the traditional approach of selecting the Hough circle with global maximum votes does not always correspond to the aorta (Fig. 2(b)). To overcome this issue, we developed a method for aorta localization using a Hough space as a medialness feature space and applying dynamic programming on that space to find the points corresponding to the center of the aorta in subsequent axial slices. The dynamic programming method was applied on the Hough spaces of subsequent axial slices to obtain a series of optimal best-fit circles for the aorta (Fig. 2(c)). In the second step, we used the estimated position and size of the aorta to detect refined aortic boundary contours. Using a polar coordinate system, the problem of finding the aortic boundary reduced to horizontal boundary detection which could be efficiently computed using the dynamic programming method. The aortic boundary was detected by computing an optimal horizontal path between the two ends of the polar image (Fig. 2(d)).

B. Intravascular Ultrasound

We have developed a computer-aided technique which allows IVUS contrast imaging to be accomplished with standard, commercially-available IVUS systems and off-the-shelf microbubble contrast agents (namely, those used for

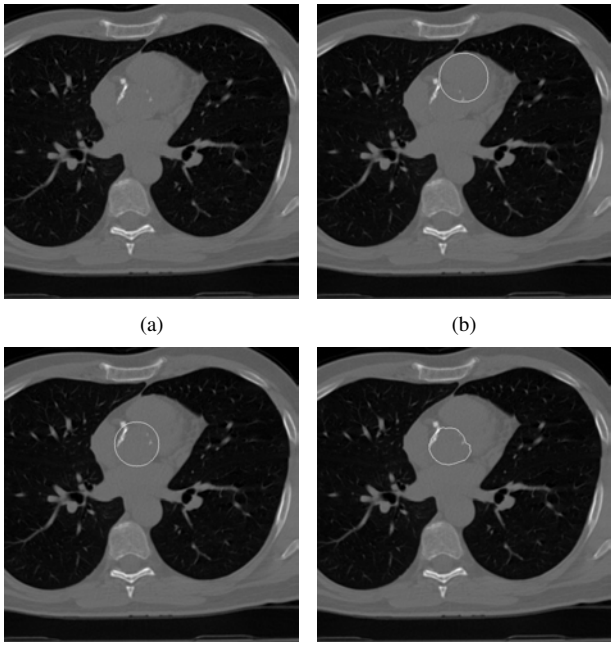

Fig. 2. (a) Original CT image, (b) aorta detected from global maximum in Hough space, (c) aorta detected using dynamic programming in Hough space, and (d) aorta boundary contour detected using dynamic programming.

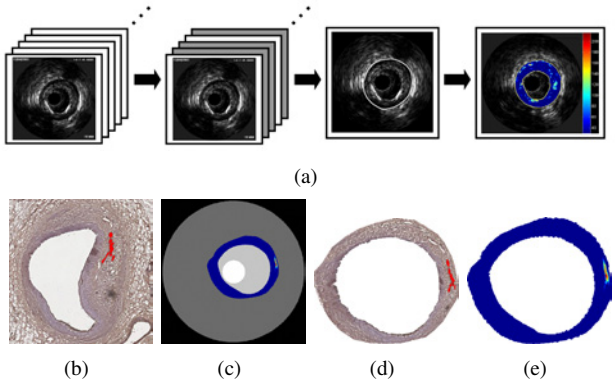

Fig. 3. Top: (a) Flowchart of an analysis of a contrast-enhanced IVUS sequence. From left to right - the original sequence, the sequence decimated by gating, the contour-tracking step, and the difference imaging and overlay of results. Bottom: Demonstration of registration between histology and IVUS. (b) A stained histological image, (c) an IVUS image to which the histology image is co-registered by manually defining corresponding landmarks, (d) deformed histology image based on the landmarks, and (e) the IVUS image highlighting the correspondence. Note the excellent agreement of our analysis with the histology.

echocardiographic purposes) [14], [15]. To this end, we have developed a method for IVUS image stabilization which enable the use of difference imaging to detect those changes which occur in the IVUS imagery due to the perfusion of an intravascularly-injected contrast agent into the plaque and vessel wall. In particular, as IVUS imaging is performed within the coronary arteries, image stabilization is required for alleviating the relative motion between the heart and the imaging catheter. The goal of image stabilization is to be able to map the pixels in a region of interest in the IVUS image from one frame to the next. Since multiple sources of motion were present, we followed three steps to detect perfusion: motion compensation, image subtraction and deriving statistics from the resulting difference images (Fig. 3(a)). If a single physiological region is mapped reliably over time, changes in its appearance can be examined by subtracting a pre-contrast baseline from a post-contrast image of that region.

However, one of the limitations of this method was related to the use of the cartesian B-mode representation of the IVUS signal. This was a disadvantage because the transformation to this representation results in loss of potentially valuable information. To overcome these limitations, we investigated the feasibility of detecting microbubbles in IVUS data by acoustic characterization of the raw IVUS data using two approaches based on one-class cost-sensitive learning [16]. In the first approach, we built a model for the microbubbles from samples of microbubbles present in the lumen during the contrast agent injection. In the second approach, we detected the microbubbles as a change from baseline IVUS data. For this, we built a model using random samples from different tissues of the vessel extracted from frames before the injection. The primary advantage of these approaches is that we made use of the raw IVUS data, thus we did not lose information contained in the radio frequency (RF) signal. The second advantage is that by using one-class learning, we did not need to provide "background" samples for building the models. In our case this was important because, although samples for microbubbles in lumen can be easily acquired by manual annotations from an expert, the background can consist of a wide variety of other imaged tissues. Thus, obtaining samples for the other tissues may be difficult and labor-intensive.

For the first approach, we obtained an average accuracy of 99.17% on the detection of microbubbles on lumen and 91.67% on the classification of pre-injection frames as having no microbubbles, with an average percentage of support vectors less than 1% of the total training samples. Figure 4 depicts the classification results on frames during injection and pre-injection. For the second approach, we obtained an average accuracy of 89.65% on the detection of baseline IVUS data and 96.78% on the classification of microbubbles as change, with an average percentage of support vectors less than 10% of the total number of samples used for training. Figure 5 depicts the classification results on frames before injection and during injection.

III. CONCLUSIONS

Our long-term goal is to develop a new risk assessment index for an individual's risk of a cardiovascular event. If this score is to be used as predictors of a future adverse event, they should provide the best representation of subclinical information. This requires optimal use of all available data. Currently, risk assessment tools do not use the wealth of information available in the images. In this paper, we presented our progress towards developing novel methods to

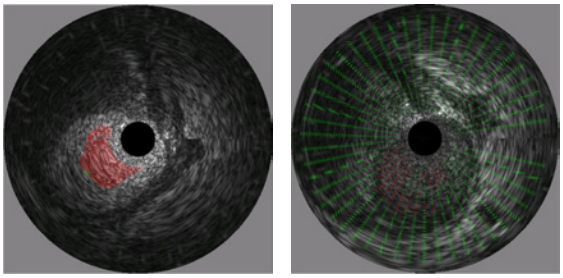

(a) (b)

Fig. 4. Classification results in (a) a frame with microbubbles in the lumen and (b) an IVUS frame before injection. In both images, the red color indicates the pixels classified as microbubbles and the green color those classified as non-microbubbles.

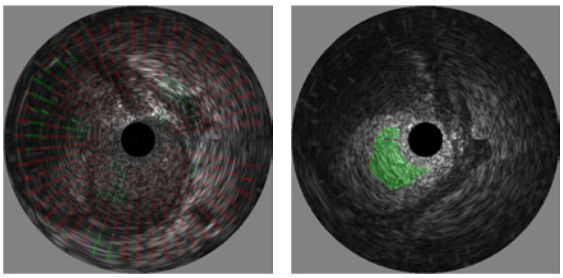

(a) (b)

Fig. 5. Classification results in (a) an IVUS frame before injection and (b) a frame with microbubbles in lumen. In both images, the red color indicates the pixels classified as baseline IVUS and the green color those classified as an anomaly.

mine information from CT and IVUS data to obtain coronary calcium and blood perfusion indicators, respectively. Our methods provided encouraging preliminary results, and opened multiple avenues for future research to achieve the final goal.

IV. ACKNOWLEDGMENTS

This work was supported in part by NIH Grant 1R21EB006829, NSF Grants IIS-0431144 and CNS-0521527, and the UH Eckhard Pfeiffer Endowment Fund. Any opinions, findings, conclusions or recommendations expressed in this material are the authors' and may not reflect the views of the sponsors.

REFERENCES

[1] National Institutes of Health, "Disease statistics," National Heart Lung and Blood Institute, Tech. Rep., 2007.

[2] M. Naghavi, P. Libby, E. Falk, S. Casscells, S. Litovsky, J. Rumberger, J. Badimon, C. Stefanadis, P. Moreno, G. Pasterkamp, Z. Fayad, P. Stone, S. Waxman, P. Raggi, M. Madjid, A. Zarrabi, A. Burke, C. Yuan, P. Fitzgerald, D. Siscovick, C. de Korte, M. Aikawa, K. Airaksinen, G. Assmann, C. Becker, J. Chesebro, A. Farb, Z. Galis, C. Jackson, I. Jang, W. Koenig, R. Lodder, K. March, J. Demirovic, M. Navab, S. Priori, M. Rekhter, R. Bahr, S. Grundy, R. Mehran, A. Colombo, E. Boerwinkle, C. Ballantyne, J. Insull, W., R. Schwartz, R. Vogel, P. Serruys, G. Hansson, D. Faxon, S. Kaul, H. Drexler, P. Greenland, J. Muller, R. Virmani, P. Ridker, D. Zipes, P. Shah, and J. Willerson, "From vulnerable plaque to vulnerable patient: A call for new definitions and risk assessment strategies: Part I," *Circulation*, vol. 108, no. 14, pp. 1664–1672, October 2003.

[3] M. Naghavi, P. Libby, E. Falk, S. Casscells, S. Litovsky, J. Rumberger, J. Badimon, C. Stefanadis, P. Moreno, G. Pasterkamp, Z. Fayad, P. Stone, S. Waxman, P. Raggi, M. Madjid, A. Zarrabi, A. Burke, C. Yuan, P. Fitzgerald, D. Siscovick, C. de Korte, M. Aikawa, K. Airaksinen, G. Assmann, C. Becker, J. Chesebro, A. Farb, Z. Galis, C. Jackson, I. Jang, W. Koenig, R. Lodder, K. March, J. Demirovic, M. Navab, S. Priori, M. Rekhter, R. Bahr, S. Grundy, R. Mehran, A. Colombo, E. Boerwinkle, C. Ballantyne, W. Insull, R. Schwartz, R. Vogel, P. Serruys, G. Hansson, D. Faxon, S. Kaul, H. Drexler, P. Greenland, J. Muller, R. Virmani, P. Ridker, D. Zipes, P. Shah, and J. Willerson, "From vulnerable plaque to vulnerable patient: A call for new definitions and risk assessment strategies: Part II," *Circulation*, vol. 108, no. 15, pp. 1772–1778, October 2003.

[4] P. Greenland, L. LaBree, S. Azen, T. Doherty, and R. Detrano, "Coronary artery calcium score combined with Framingham score for risk prediction in asymptomatic individuals," *Journal of the American Medical Association*, vol. 291, no. 2, pp. 210–215, 2004.

[5] L. Shaw, P. Raggi, E. Schisterman, D. Berman, and T. Callister, "Prognostic value of cardiac risk factors and coronary artery calcium screening for all-cause mortality," *Radiology*, vol. 228, no. 3, pp. 826–833, 2003.

[6] A. Taylor, J. Bindeman, I. Feuerstein, F. Cao, M. Brazaitis, and P. O'Malley, "Coronary calcium independently predicts incident premature coronary heart disease over measured cardiovascular risk factors: Mean three-year outcomes in the Prospective Army Coronary Calcium (PACC) project," *Journal of the American College of Cardiology*, vol. 46, no. 5, pp. 807–814, 2005.

[7] N. D. Wong, M. J. Budoff, J. Pio, and R. C. Detrano, "Coronary calcium and cardiovascular event risk: Evaluation by age- and sex-specific quartiles," *American Heart Journal*, vol. 143, no. 3, pp. 456–459, 2002.

[8] N. Rodondi, B. C. Taylor, D. C. Bauer, L. Y. Lui, M. T. Vogt, H. A. Fink, W. S. Browner, S. R. Cummings, and K. E. Ensrud, "Association between aortic calcification and total and cardiovascular mortality in older women," *Journal of Internal Medicine*, vol. 261, no. 3, pp. 238–244, 2007.

[9] J. C. Witteman, F. J. Kok, J. L. van Saase, and H. A. Valkenburg, "Aortic calcification as a predictor of cardiovascular mortality," *Lancet*, vol. 2, no. 8516, pp. 1120–1122, 1986.

[10] M. Gossl, N. Malyar, M. Rosol, P. Beighley, and E. Ritman, "Impact of coronary vasa vasorum functional structure on coronary vessel wall perfusion distribution," *American Journal of Physiology - Heart and Circulatory Physiology*, vol. 285, no. 5, pp. H2019–H2026, 2003.

[11] U. Kurkure, D. Chittajallu, G. Brunner, R. Yalamanchili, and I. Kakadiaris, "Detection of coronary calcifications using supervised hierarchical classification," in *Proc. Medical Image Computing and Computer-Assisted Intervention Workshop on Computer Vision for Intravascular and Intracardiac Imaging*, New York, NY, Sep. 10 2008.

[12] G. Brunner, D. Chittajallu, U. Kurkure, and I. Kakadiaris, "A heart-centered coordinate system for the detection of coronary artery zones in non-contrast Computed Tomography data," in *Proc. Medical Image Computing and Computer-Assisted Intervention Workshop on Computer Vision for Intravascular and Intracardiac Imaging*, New York, NY, Sep. 10 2008.

[13] U. Kurkure, O. Avila-Montes, and I. Kakadiaris, "Automated segmentation of thoracic aorta in non-contrast CT images," in *Proc. IEEE International Symposium on Biomedical Imaging: From Nano to Macro*, Paris, France, May 14-17 2008.

[14] S. M. O'Malley, M. Vavuranakis, M. Naghavi, and I. A. Kakadiaris, "Intravascular ultrasound-based imaging of vasa vasorum for the detection of vulnerable atherosclerotic plaque," in *Proc. Medical Image Computing and Computer-Assisted Intervention*, Palm Springs, California, USA, October 2005, pp. 343–351.

[15] S. M. O'Malley, M. Naghavi, and I. A. Kakadiaris, "One-class acoustic characterization applied to blood detection in IVUS," in *Proc. Medical Image Computing and Computer-Assisted Intervention*, Brisbane, Australia, 2007, pp. 202–209.

[16] E. Mendizabal-Ruiz and I. A. Kakadiaris, "One-class acoustic characterization applied to contrast agent detection in IVUS," in *Proc. Medical Image Computing and Computer-Assisted Intervention Workshop on Computer Vision for Intravascular and Intracardiac Imaging*, New York, NY, Sep. 10 2008.